Implementation of a module for risk of ozone impacts assessment to vegetation in the Integrated Assessment Modelling system for the Iberian Peninsula. Evaluation for wheat and Holm oak

Juan Manuel de Andrés , Rafael Borge, David de la Paz, Julio Lumbreras, Encarnación Rodríguez

A B S T R A C T

A module to estimate risks of ozone damage to vegetation has been implemented in the Integrated Assessment Modelling system for the Iberian Peninsula. It was applied to compute three different indexes for wheat and Holm oak; daylight AOT40 (cumulative ozone concentration over 40 ppb), cumulative ozone exposure index according to the Directive 2008/50/EC (AOT40-D) and POD_Y (Phytotoxic Ozone Dose over a given threshold of Y nmol m^{-2} s^{-1}). The use of these indexes led to remarkable differences in spatial patterns of relative ozone risks on vegetation. Ozone critical levels were exceeded in most of the modelling domain and soil moisture content was found to have a significant impact on the results. According to the outputs of the model, daylight AOT40 constitutes a more conservative index than the AOT40-D. Additionally, flux-based estimations indicate high risk areas in Portugal for both wheat and Holm oak that are not identified by AOT-based methods.

1. Introduction

Tropospheric ozone (O_3) is a secondary air pollutant formed as a result of complex photochemical reactions between nitrogen oxides, volatile organic compounds and other precursors (Atkinson, 2000) and it is one of the air pollutants of most concern in Europe (EEA, 2010). It is a strong photochemical oxidant that may cause serious health problems as well as damage to materials and vegetation by producing visible leaf injury as well as growth and yield reductions (Ashmore, 2005; Delgado-Saborit and Esteve-Cano, 2008; Fumagalli et al., 2001).

Over the last two decades, the effects of ground-level ozone on plants have led to a request from policy makers to scientists for methods to quantify the risk of damage to vegetation (Fuhrer and Booker, 2003; Simpson et al., 2007). As a result, intensive work is being carried out to develop quantitative methods for this purpose (e.g. Alonso et al., 2008; Mills et al., 2007a, 2011a; Pleijel et al., 2004, 2007).

The cumulative exposure parameter AOT40 (Accumulated Ozone concentration over a Threshold of 40 parts per billion), has been extensively used under the framework of the United Nations Economic Commission for Europe (UNECE) Convention on Long-Range Transboundary Air Pollution (CLRTAP) as the concentration-based descriptor of ozone effects on vegetation (LRTAP Convention, 2010) to inform air pollution abatement policies (Baumgarten et al., 2009; Denby et al., 2010; Sanz et al., 1999). It is calculated as follows:

$$\mathrm{AOT40} = \sum_{\textit{accumulation period}} \max(0; C_C - 40)\Delta t \quad (1)$$

where C_C is the hourly mean ozone concentration (in ppb) at canopy height and $\Delta t = 1$ h.

The AOT40 concept is also considered by the European legislation to establish ozone target values and long-term objectives for the protection of vegetation. In this contribution, the AOT40 computed according to CLRTAP and according to the Directive 2008/50/EC will be referred to as daylight AOT40 and AOT40-D, respectively. The differences between these two metrics are related to the accumulation period and reference height for O_3 concentration values, as explained Section 2.

The exposure-based approach has important limitations and uncertainties because it only considers the ozone concentration, not the actual flux or dose of ozone entering the plant (Mills et al., 2007a). To solve these problems, the flux-based approach was developed under the CLRTAP framework taking into account the influence of different parameters affecting the ozone uptake

mechanism (such as temperature, water vapour pressure deficit -VPD-, light, etc.) apart from ozone concentration to estimate the amount of ozone entering the plant through the stomata (Emberson et al., 2000; LRTAP Convention, 2010; Nussbaum et al., 2003; Tuovinen et al., 2004).

This alternative approach is biologically more relevant because stomatal uptake (Phytotoxic Ozone Dose, POD_Y) is the only pathway through which toxicologically relevant ozone molecules penetrate leaf tissue (Zhang et al., 2006). The POD_Y is defined as (ICP Vegetation 2009; LRTAP Convention, 2010):

$$POD_Y = \sum_{accumulation\ period} \max(0; F_{st} - Y)\Delta t \quad (2)$$

where F_{st} is the stomatal ozone flux per projected leaf area (PLA) to sunlit leaves at the canopy top and Y is the threshold stomatal flux per PLA (in nmol m^{-2} s^{-1}).

Since the 1980s, much progress has been made in establishing ozone Critical Levels (CL) for vegetation (Mills et al., 2007b). In the summer of 2010 the ICP Vegetation (International Cooperative Programme on Effects of Air Pollution on Natural Vegetation and Crops) has released a new version of the "Chapter 3: Mapping critical levels for vegetation" as part of the modelling and mapping manual of the LRTAP Convention (LRTAP Convention, 2010). In this chapter, the CLs for vegetation were defined as the "concentration, cumulative exposure or cumulative stomatal flux of atmospheric pollutants above which direct adverse effects on sensitive vegetation may occur according to present knowledge". So far, CLs have only been defined for a few types of crops, forest trees and semi-natural vegetation.

In the Mediterranean region, especially in summer, weak levels of Azores anti-cyclonic subsidence, low winds, and strong insulation favour photochemical production of O_3 with development of mesoscale processes and recirculation within air masses (Millán et al., 2000). As a result of that, ambient O_3 concentrations can reach concentrations high enough to produce phytotoxic effects in native vegetation and crops (Sanz et al., 2007). Evidences of O_3 injury in this area are reported elsewhere (Paoletti, 2006; Sanz et al., 2000). However, relationships between O_3 exposure and effects on vegetation often fail. This discrepancy can be partially explained by the sclerophyll character of the vegetation in Mediterranean ecosystems, characterized by low foliar gas exchange rates and their active antioxidant pool (Elvira et al., 2004; Paoletti, 2006).

The exceedance of CL of ozone in the Mediterranean area might largely differ depending on the approach used for the risk assessment of ozone damage. According to Alonso et al. (1999) and Fumagalli et al. (1999), in Southern Europe, namely Spain and Italy, yield losses predicted through the flux approach are smaller than losses indicated by the ozone response functions based on the daylight AOT40 index proposed by Fuhrer et al. (1997). The highest ozone concentrations in these areas occur when sunny and dry weather provides favourable conditions for the formation of ozone (Dueñas et al., 2002; García et al., 2005). However, under these conditions non-irrigated vegetation experiences high soil moisture deficits (SMDs) resulting in reduced stomatal conductance and hence low ozone flux (Emberson et al., 2000). It is therefore important to understand the differences that may arise from alternative methods to evaluate potential ozone impacts on vegetation, especially in the context of the particular climatic characteristics of the Mediterranean region, with summers under the influence of the Azores anticyclone, strong insulation, high temperatures and periods of drought (Mediavilla and Escudero, 2004).

This contribution discusses the implementation of the methodology developed and used within the framework of the UNECE CLRTAP (LRTAP Convention, 2010) to assess the risk of ozone impacts to vegetation, extending the capabilities of the Integrated Assessment Modelling (IAM) system for the Iberian Peninsula (Borge et al., 2009, 2010), a system intended to assist policy makers in the assessment and comparison of environmental policies and control strategies in Spain based on emission projections (Lumbreras et al., 2008). This system also constitutes the basis for health impact assessments recently carried out in Spain (Boldo et al., 2011). This work allows estimating and comparing the risk of ozone damage on vegetation in the Iberian Peninsula (IP) and Balearic Islands through concentration-based and flux-based approaches integrating both, modelled meteorological conditions and O_3 levels. Such development establishes a framework for estimating the risk of ozone impacts on vegetation under different emission/policy scenarios according to the concentration–response and flux–response relationships derived from experimental studies (Fuhrer et al., 1997; Karlsson et al., 2004; Mills et al., 2007a, 2011a; LRTAP Convention, 2010; Pleijel et al., 2004).

Special attention is given to the analysis of the influence of the soil moisture content (SMC) on the results of the modelling system, since the stomatal conductance may be largely overestimated at sites under drought stress otherwise (Alonso et al., 2008).

The risk assessment performed in this study is restricted to wheat (extensively cultivated in the IP) and Holm oak (the most representative of all Mediterranean evergreen broadleaf species).

2. Methodology

2.1. Air quality modelling system

The air quality modelling system relies on the Community Multiscale Air Quality (CMAQ) model (Byun and Ching, 1999; Byun and Schere, 2006), a state-of-the-art Eulerian chemistry transport model based on the one-atmosphere paradigm, widely used worldwide to investigate tropospheric ozone (e.g., Brankov et al., 2003; Xu et al., 2008; Shi et al., 2009). Emissions are taken from an emission model based on the Sparse Matrix Operator Kernel Emissions (SMOKE) modelling system (UNC Carolina Environmental Program, 2005) as described in Borge et al. (2008a).

The model selected to provide the meteorological fields required by the chemical-transport model (CMAQ) and the emission processing system (SMOKE) is the Weather Research and Forecasting (WRF) modelling system (Skamarock and Klemp, 2008). This non-hydrostatic mesoscale model constitutes a state-of-the-art atmospheric simulation system based on the Fifth-Generation Penn State/NCAR Mesoscale Model (MM5) (Grell et al., 1994). Meteorological fields from WRF are consistently used for the computation of the variables involved in the flux-based method as well. A detailed description of the initialization and set-up of the WRF model for the IP can be found in Borge et al. (2008b).

The transport-chemistry model used in this application was CMAQ v4.6. Atmospheric chemistry was simulated through the Carbon Bond CB05 mechanism (Yarwood et al., 2005), a lumped structure chemical mechanism including 156 reactions and 69 species including aerosols. Further information on emissions processing and other model options can be found in Borge et al. (2008a) and Borge et al. (2010) respectively.

2.2. Modelling domain

Simulated meteorology and O_3 concentration values are based on a nested approach. The area of study corresponds to the innermost rectangle in Fig. 1a, a modelling domain centred over the IP with 75 columns and 60 rows of 16×16 km^2 grid cells (1200×960 km^2). Dynamic boundary conditions are provided by the GEOS-Chem global chemical-transport model (Bey et al., 2001). Details about the model vertical structure (30 layers, 5 of them in the first 100 m) and boundary conditions can be found in Borge et al. (2010). The mesoscale modelling system WRF-CMAQ was run for the year 2007 with 1 h temporal resolution.

2.3. Land use and soil types

The distribution of wheat and Holm oak within the studied area was determined through the CORINE Land Cover 2000 (CLC2000, http://sia.eionet.europa.eu/CLC2000) database, which provides consistent information of land-use across Europe. The spatial distribution of these species is shown in Fig. 2. Soil types, textures and soil physical parameters in this study are based on the Global 2-minute, 19-category United Nation FAO (Food and Agricultural Organization) + STATSGO soil

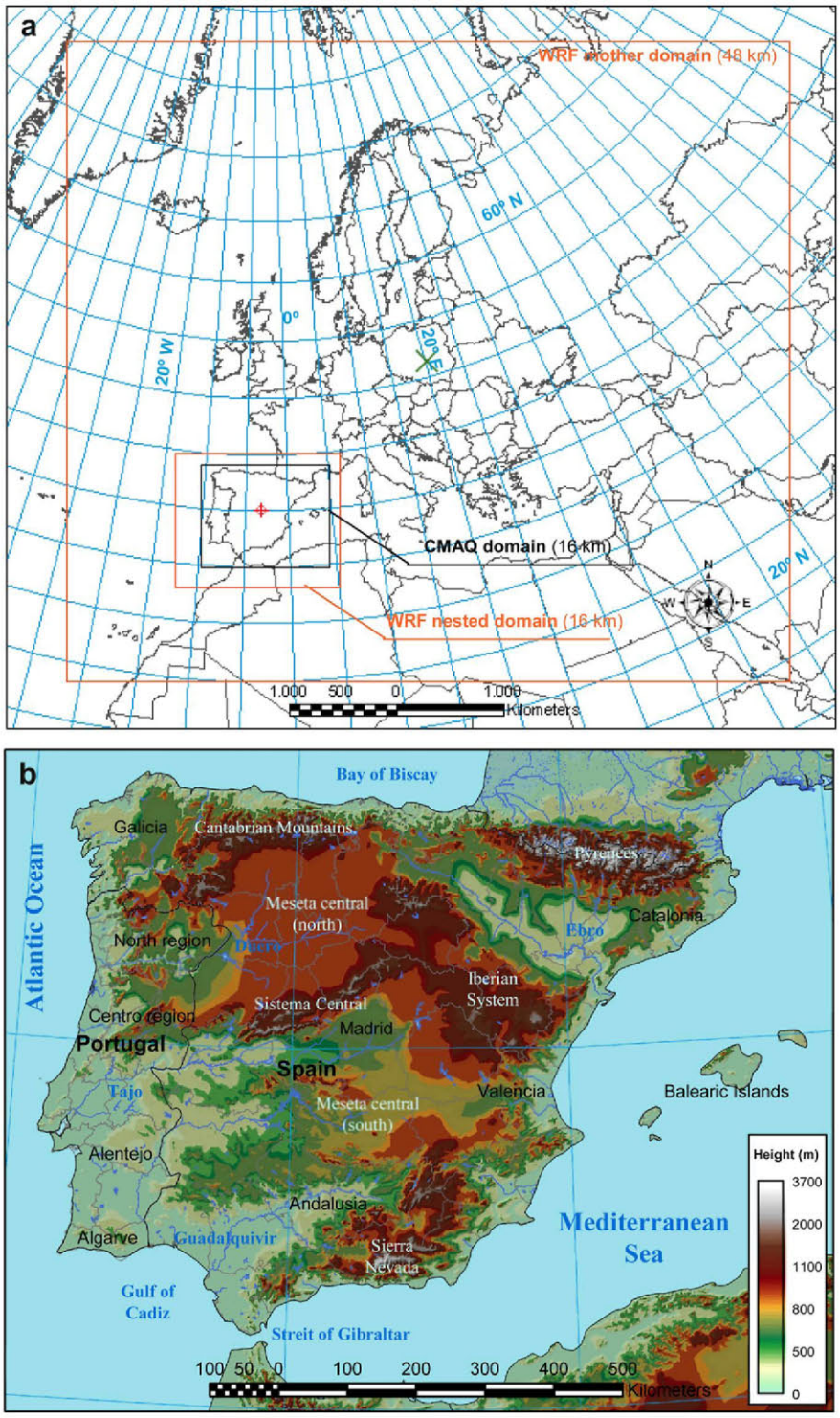

Fig. 1. Modelling domains (Lambert Conformal projection). The rectangles in orange represent the WRF domains (a) and detail of the CMAQ modelling domain (b). (For interpretation of the references to colour in this figure legend, the reader is referred to the web version of this article.)

data available at WRF user's site (http://www.mmm.ucar.edu/wrf/users/download/get_sources.html).

2.4. Estimation of exposure-based and flux-based metrics

Daylight AOT40, AOT40-D and POD_Y were calculated from hourly ozone concentration outputs of the CMAQ model. Conversion of ozone concentration modelled by CMAQ at the height of the centre of the appropriate layer to that at the top of the canopy was carried out by means of the *Tabulated gradient method* (LRTAP Convention, 2010). Concretely, conversion from 4 m height above the ground (first CMAQ layer) to 1 m height above the ground was carried out for wheat. No conversion was necessary for Holm oak since the second vertical layer in CMAQ corresponds to 15 m height above the ground, coinciding with canopy height. The results shown, compared and discussed below were calculated over different accumulation periods, depending on the metric.

2.4.1. Daylight AOT40

The daylight AOT40 index should be calculated for daylight hours (global radiation >50 W m^{-2}) during the growth period of the receptor and using ozone concentration at canopy height. An accumulation period of three months, from 1

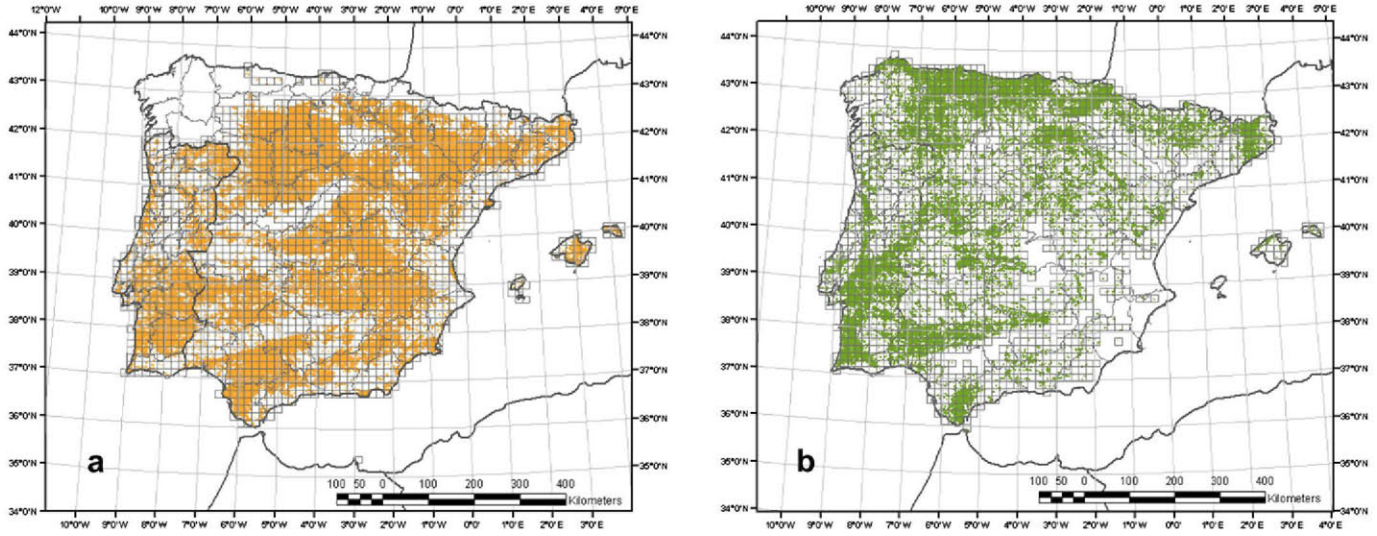

Fig. 2. Spatial distribution assumed for wheat (a) and Holm oak (b) and overlap with the model grid. 1861 and 1810 grid cells are intersected respectively.

April to 30 June (Mills et al., 2007a), was assumed for wheat (time period centred on the estimated date for anthesis). Following LRTAP Convention (2010) recommendations for the Mediterranean evergreen forests, a continuous accumulation period (whole year) was assumed for Holm oak if night temperatures do not fall below −4 °C. Otherwise, an onset of growing season was assumed when the night temperatures rise above −4 °C for 5 consecutive nights and a cessation of growing season was assumed when such temperatures fall below −4 °C for 5 days.

2.4.2. AOT40-D

The AOT40 according to the Directive 2008/50/EC is estimated using hourly ozone concentration values measured or modelled between 8:00 and 20:00 (Central European Time). The accumulation period for AOT40-D metric is different from that of daylight AOT40, being from 1 May to 31 July for vegetation protection and from 1 April to 30 September for forests protection (the latter is not explicitly used for the definition of target values or long-term objectives but it is mentioned in the Directive and is coincident with the default exposure window for the accumulation of AOT40 suggested by LRTAP Convention (2010) for all deciduous and evergreen species in all regions throughout Europe). Some of the differences found between daylight AOT40 and AOT40-D metrics can be explained by these different accumulation periods.

2.4.3. POD_Y

The POD_Y was calculated according to the formulation and criteria of the LRTAP Convention (2010). The stomatal conductance was determined as follows:

$$g_{sto} = g_{max} * \left[\min\left(f_{phen}, f_{O_3}\right)\right] * f_{light} * \max\left\{f_{min}, \left(f_{temp} * f_{VPD} * f_{SWP}\right)\right\} \quad \text{for forests} \tag{3}$$

$$g_{sto} = g_{max} * \left[\min\left(f_{phen}, f_{O_3}\right)\right] * f_{light} * \max\left\{f_{min}, \left(f_{temp} * f_{VPD} * f_{PAW}\right)\right\} \quad \text{for crops} \tag{4}$$

where g_{sto} is the actual stomatal conductance (mmol O_3 m^{-2} PLA s^{-1}) and g_{max} is the species-specific maximum stomatal conductance (mmol O_3 m^{-2} PLA s^{-1}). The other parameters, representing phenological changes (f_{phen}), photosynthetic active radiation (f_{light}), air temperature (f_{temp}), vapour pressure deficit (f_{VPD}), soil water potential (f_{SWP}) or plant available water (f_{PAW}) and the relative minimum g_{sto} that occurs during daylight hours (f_{min}), are expressed in relative terms as a proportion of g_{max} (values between 0 and 1).

The accumulation period used for the flux-based approach for wheat began 200 °C days before mid-anthesis (full flowering) and finished 700 °C days after mid-anthesis. The mid-anthesis was estimated using a temperature sum of 1075 °C days after 1 January (if temperature exceeded 0 °C on that date) or after the first date of the year when the temperature exceeded 0 °C. For Holm oak, a year round growing season was assumed (LRTAP Convention, 2010).

The species-specific threshold values (Y) and the rest of the parameters used in this study are shown in Table 1. Most of parameters were computed from basic meteorological WRF outputs (mainly relative humidity, temperature and radiation). The SMC was estimated with the help of the Noah Land Surface Model (LSM) (Chen and Dudhia, 2001a, 2001b) implemented in WRF. The Noah LSM uses the water content form of the Richards equation (Richards, 1931) and distinguishes 4 soil layers and 19 different soil types. The thickness of each layer from the ground surface to the bottom is 0.1, 0.3, 0.6, and 1.0 m, respectively (total soil depth of 2 m). According to LRTAP Convention (2010), f_{PAW} was estimated from the SMC and from the field capacity and the wilting point of the soil profile (soil type depending

Table 1
Parameterization used for the O_3 flux-based model simulation for wheat and Holm oak (LRTAP Convention, 2010). Estimation of risk of ozone damage within Integrated Assessment Modelling.

Parameter	Units	Wheat	Holm oak
g_{max}	mmol O_3 m^{-2} (PLA) s^{-1}	500	180
f_{min}	(fraction)	0.01	0.02
SGS	year day	–	1 (1 Jan)
EGS	year day	–	365 (31 Dec)
f_{phen_limA}	year day	–	80 (21 Mar)
f_{phen_limB}	year day	–	320 (16 Nov)
f_{phen_a}	(fraction)	0.3	1.0
f_{phen_b}	(fraction)	0.7	1.0
f_{phen_c}	(fraction)	–	0.3
f_{phen_d}	(fraction)	–	1.0
f_{phen_e}	°C days/fraction	200	1.0
f_{phen_f}	°C days	0	–
f_{phen_g}	°C days	100	–
f_{phen_h}	°C days	525	–
f_{phen_i}	°C days	700	–
f_{phen_2}	days	–	130
f_{phen_3}	days	–	60
light_a	dimensionless	0.0105	0.012
T_{min}	°C	12	1
T_{opt}	°C	26	23
T_{max}	°C	40	39
VPD_{max}	kPa	3.1	2.2
VPD_{min}	kPa	4.8	4.0
$\sum VPD_{crit}$ [a]	kPa	8	–
PAW_t	%	50	–
SWP_{max}	MPa	–	−1.0
SWP_{min}	MPa	–	−4.5
f_{O_3}	POD_0, mmol m^{-2} s^{-1}	14	–
f_{O_3}	(exponent)	8	–
Y	nmol O_3 m^{-2} PLA s^{-1}	6	1
h	m	1	15
L	cm	2	5.5

g_{max}, maximum stomatal conductance; f_{min}, minimum daytime stomatal conductance; SGS, day of the year at the start of the growing season; EGS, day of the year at the end of the growing season; f_{phen}, function for variation in stomatal conductance with leaf/needle age (subscripts a–i; 2,3 to solve the function during the time); light_a, specie-specific coefficient; $T_{min/opt/max}$, minimum/optimum/maximum leaf temperature at which stomatal opening occurs; $VPD_{max/min}$, maximum/minimum water vapour pressure déficit; PAW_t, threshold of rootzone Plant Available Water above which stomatal conductance is at a maximum; $SWP_{max/min}$, maximum/minimum soil water potential; f_{O_3}, function for variation in stomatal conductance via the onset of early senescente; Y, ozone stomatal flux rate threshold; h, average canopy height; L, cross-wind leaf dimension.

[a] If ΣVPD (calculated for each daylight hour until the dawn of the next day) is larger than or equal to ΣVPD_{crit}, the stomatal conductance (g_{sto}) is valid if it is smaller or equal to the g_{sto} value of the preceding hour. Otherwise, g_{sto} is replaced by the g_{sto} of the preceding hour in the estimation of stomatal conductance.

parameters). For f_{PAW} calculation (parameter used for wheat), the SMC was obtained as a weighted mean from the three first soil layer (i.e. 0–100 cm depth), considering their specific SMC and thickness. Although most of the wheat root length density is located in the first 0.5 m of the soil, the wheat roots easily reach beyond 1 m depth (Li et al., 2010; Lilley and Kirkegaard, 2011). On the other hand, f_{SWP} (parameter used for Holm oak) was calculated from the soil water potential, computed from the SMC according to Chen and Hu (2004) (Eq. (5)).

$$\Psi(\Theta) = \frac{\Psi_s}{(\Theta/\Theta_s)^b} \tag{5}$$

where Ψ is the soil water potential, Θ is the soil water content, Ψ_s is the saturation soil potential, Θ_s is the saturation soil moisture content, and b is the curve fitting parameter that relates soil water potential and water content (the last tree parameters depending on soil type). Likewise, SMC for the f_{SWP} parameter is derived from soil-layer specific SMC, but considering the four layers in the Noah LSM (up to 2 m depth) since Holm oak roots can reach even higher depths (Moreno et al., 2005).

2.5. Exceedance of Critical Level (CL)

The concept of relative exceedance (R_{exc}) introduced by Simpson et al. (2007) was used to evaluate the exceedance of CL throughout the domain (Eq. (6)). This metric refers to CL and therefore allows a consistent comparison of daylight AOT40 and POD_Y values.

$$R_{exc} = \frac{M}{CL_M} \tag{6}$$

where the appropriate CL values are used as a normalizing factor, and M is the metric (daylight AOT40 or POD_Y) with critical level CL_M.

As for the AOT40-D, target values (TV) are used as normalizing factor since the critical level concept is not used for this index. The meaning of R_{exc} is however equivalent. CL_M and TV values used in this study are summarized in Table 2.

$$R_{exc} = \frac{M}{TV} \tag{7}$$

Exceedance of the CL and TV was calculated only for wheat because there are insufficient data available to derive neither a critical level specific for trees in the Mediterranean area (LRTAP Convention, 2010; Mills et al., 2011a) nor a specific target value for forests (Directive 2008/50/EC).

2.6. Influence of the Soil Moisture Content (SMC)

For the evaluation of the influence of SMC the model was run twice for both wheat and Holm oak. In the first run, the f_{PAW} and the f_{SWP} parameters were set equal to 1, i.e., the effect of SMC was neglected. In the second run, the LRTAP Convention (2010) methodology was used to estimate f_{PAW} and f_{SWP}. Finally, to carry out the evaluation of the SMC influence on the results, the metric Soil Moisture Content effect (SMC_{effect}) was used.

For wheat, the SMC_{effect} was estimated according to Eq. (8)

$$SMC_{effect(wheat)} = \frac{POD_6(f_{PAW} = 1) - POD_6(f_{PAW})}{CL_M} \tag{8}$$

where CL_M is the flux-based critical level for wheat (Table 2), the term $POD_6(f_{PAW} = 1)$ is the POD_6 when SMC is neglected and $POD_6(f_{PAW})$ is the POD_6 resulting when the influence of SMC is taken into account.

As no flux-based CL is defined for Holm oak yet, the SMC_{effect} was estimated according to Eq. (9)

Table 2
Metrics, critical levels, target values and accumulation periods used for different types of vegetation.

	Metric	Critical level (CL_M)/ Target value (TV)[a]	Accumulation period
Wheat	AOT40	3 ppm h	1 April–30 June
Wheat	AOT40 (Directive)	18,000 μg/m^3 $h \approx 9$ ppm h	1 May–31 July
Wheat	POD_6	1 mmol m^{-2}	200 °C days before anthesis to 700 °C days after anthesis
Holm oak	AOT40	–	whole year
Holm oak	AOT40 (Directive)	–	1 April–30 September
Holm oak	POD_1	–	whole year

[a] CL values according to LRTAP Convention (2010). In the case of the Directive 2008/50/EC, the TV referrers to a target value.

$$SMC_{effect(Holm\ oak)}(\%) = \left(\frac{POD_1(f_{SWP} = 1) - POD_1(f_{SWP})}{POD_1(f_{SWP} = 1)}\right) \times 100 \tag{9}$$

where the term $POD_1(f_{SWP} = 1)$ is the POD_1 when SMC is neglected and $POD_1(f_{SWP})$ is the POD_1 when the influence of SMC is taken into account.

In order to gain a better understanding of the role of SMC in the risk assessment, four locations were selected for a comprehensive analysis (Fig. 7). Location 1 is representative of those locations where there is a differential effect of SMC between wheat and Holm oak. This can be explained because of the high SMC of the deepest soil layer which differs from that of the three superficial layers. In this case, during the accumulation period defined for wheat, SMC has a strong impact on f_{PAW} but a limited one on f_{SWP} since there is water available at the bottom of the profile. Location 3 represents a situation where SMC variations are consistent throughout the whole soil profile and therefore, f_{PAW} and f_{SWP} evolve in a similar way. Location 2 is representative of areas with strong water deficit over most of the accumulation period (dry location) while location 4 illustrates the behaviour of the main parameters for no-drought conditions (wet location).

3. Results and discussion

Exposure and flux-based assessments of potential ozone damages on vegetation in the IP have been performed following the methodology described. In this section, the resulting maps for daylight AOT40, AOT40-D and POD_Y are shown and discussed.

A common colour scale, based on the 10 deciles of the grid-data distribution has been used to present the results. This representation allows a straightforward interpretation of the spatial variability between exposure and flux-based approaches.

3.1. CMAQ model evaluation

Some references regarding CMAQ model performance and reliability are presented. Model O_3 concentration outputs were compared with observations from 12 rural background monitoring stations from the European Air quality dataBase (AirBase), 9 of them belonging to the EMEP network. Fig. 3a shows AOT40 values predicted by the chemical-transport model along with the location of the air quality monitoring stations selected and the corresponding AOT40 observed values. Fig. 3b shows the AOT40 values predicted by the EMEP model (Benedictow et al., 2010) used for similar assessment at European scale (Simpson et al., 2003). A direct comparison of model results is not straightforward since both models differ substantially in spatial and vertical resolution. In order to provide an insight of the differences in O_3 predictions at surface level, CMAQ predictions (16×16 km^2) have been averaged over EMEP 50×50 km^2 grid cells. The comparison is illustrated in Fig. 3c. The overall average AOT40 predicted by both models is rather similar (6.0 and 5.9 ppm h for EMEP and CMAQ respectively) although there is not a clear pattern on the distribution of relative errors (the distribution of dots at both sides of the 1:1 line is rather balanced).

A complete statistical analysis of the CMAQ model performance is summarized in Table 3, following the guidelines from the recent activities of FAIRMODE subgroup 4 (Thunis et al., 2011; Pederzoli et al., 2011). In addition, the mean normalized bias and error (MNB and MNE), used for the classic US EPA's ozone performance recommendations (Russell and Dennis, 2000) are included. As reported in previous studies (e.g. Appel et al., 2007; Borge et al., 2010) the CMAQ model tends to overpredict low O_3 concentration values, but exhibits a satisfactory global performance with a mean normalized bias below 15% for all the monitoring stations. Global indexes for all the metrics analyzed are within the recommended ranges.

3.2. Wheat

Results for daylight AOT40, AOT40-D and POD_6 values for wheat are shown in Fig. 4. The daylight AOT40 index (Fig. 4a) reaches

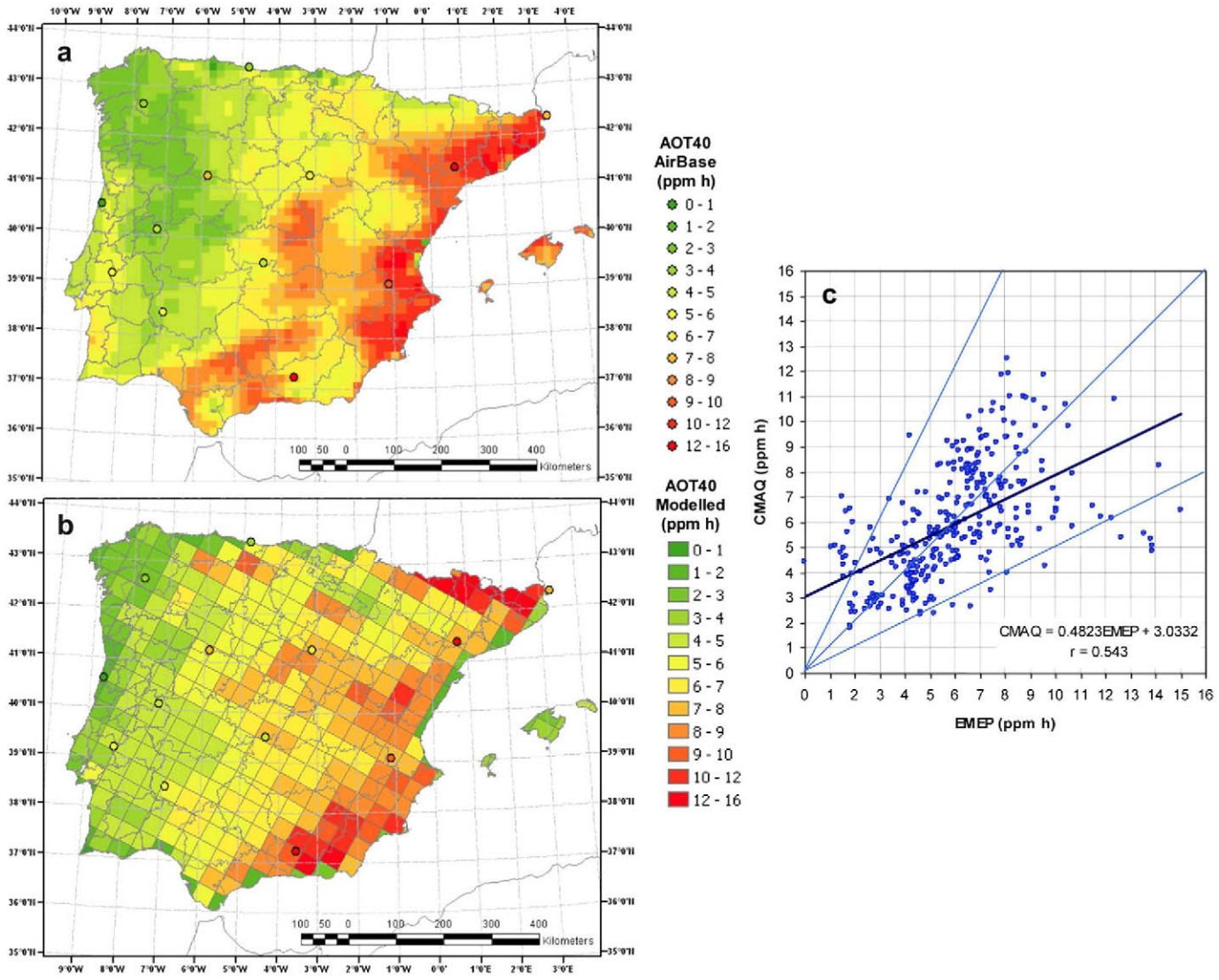

Fig. 3. CMAQ (a) and EMEP (b) modelled AOT40 values for the modelling domain. The circles represent the 12 AirBase monitoring stations used for model evaluation. AOT40 from AirBase, EMEP and CMAQ are estimated using a default accumulation period of May–July. For AirBase, AOT40 values are based on ozone concentrations at measurement height (usually 3 m). For EMEP and CMAQ, AOT40 values are based on ozone concentration referred to 1 m height. Comparison of CMAQ and EMEP AOT40 estimates (c).

maximum values in the eastern and north eastern area of Spain. In contrast, wheat crops located in Portugal and most of the southern central plateau (Meseta Central) are exposed to lower AOT40 levels, below the median. The AOT40-D index (Fig. 4c), shows a rather different picture extending the highest risks areas to the central and southern IP. These differences arise from the different accumulation periods of these two metrics.

The information provided by the cumulative flux uptake map is shown in (Fig. 4e). Likewise exposure-based methods, high relative risks of damage are found in the North eastern coastal areas and in the Ebro Valley. However, estimated risk through exposure and flux-based approaches largely differ all over the coast of Portugal and the lower Tajo Valley. As shown in Fig. 4e, ozone uptakes are lower in the centre of the IP. These results are consistent with those obtained at European scale by Simpson et al. (2007) and the assessment of Mills et al. (2011b) for generic crops. The POD_6 spatial distribution fits quite well with visible injury data attributed to ozone on crops, shrubs and semi-natural vegetation species according to ICP Vegetation (2007).

As it can be seen in Fig. 4a and e, values of AOT40 between 9.5 and 12.5 ppm h and values of POD_6 between 7.5 and 8.5 mmol m^{-2} PLA were found is some areas of the IP. According to the corresponding response functions in LRTAP Convention (2010), yield losses of up to 20% and 30%, respectively might be expected in such locations.

Regarding exceedances of CL, it can be observed that values of R_{exc} for the daylight AOT40 metric are usually larger than 1 (Fig. 4b). Daylight AOT40 values are 1–3 times larger than the critical level in most of the Peninsula (90% grid cells containing wheat crops). In the case of R_{exc} for AOT40-D metric, the values are lower than 1 in most of the wheat area (85% grid cells) and only the eastern part of the IP and a few locations in the centre and south exceed this value. According to these results, daylight AOT40 constitutes a more conservative index than the AOT40-D since R_{exc} values obtained for daylight AOT40 are higher. As far as POD_6 is concerned, CL is amply exceeded with R_{exc} between 4 and 6 in 61% of grid cells and R_{exc} higher than 6 in 33% of grid cells (Fig. 5a).

Following the LRTAP Convention (2010) recommendations, these results were obtained using VPD_{max} and VPD_{min} values suggested for specific application under Mediterranean conditions (VPD_{max} = 3.1 kPa and VPD_{min} = 4.8 kPa), which are based on field experiments performed in central Spain for four years (Gonzalez, in

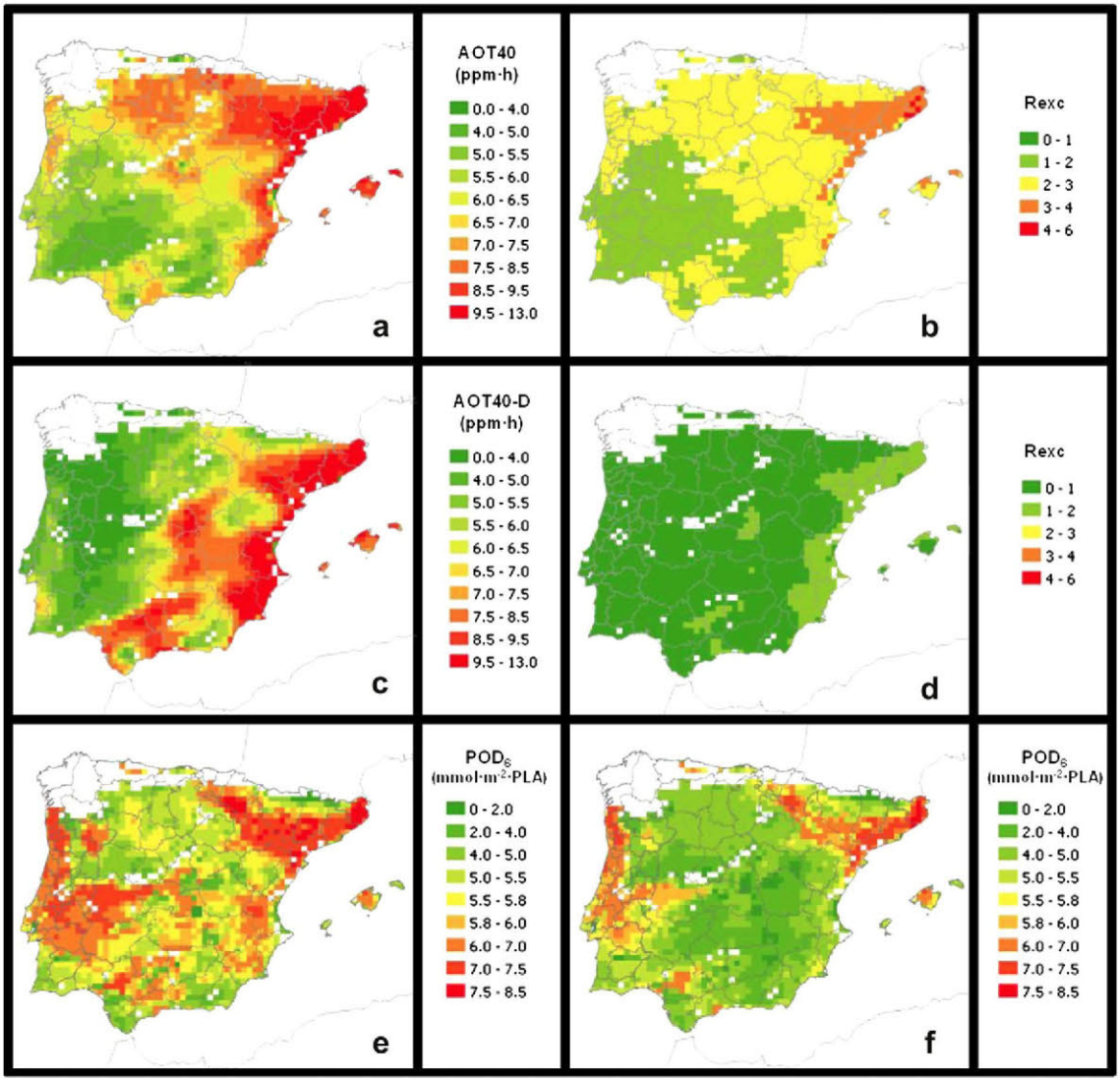

Fig. 4. Distribution of AOT40 (a), AOT40-D (c) and POD_6 (e) values during 2007 in the Iberian Peninsula for wheat. Exceedances of the different metrics over CL according to AOT40 (b), and AOT40-D (d). Distribution of POD_6 values taking into account VPD_{max} = 1.2 kPa and VPD_{min} = 3.2 kPa (f).

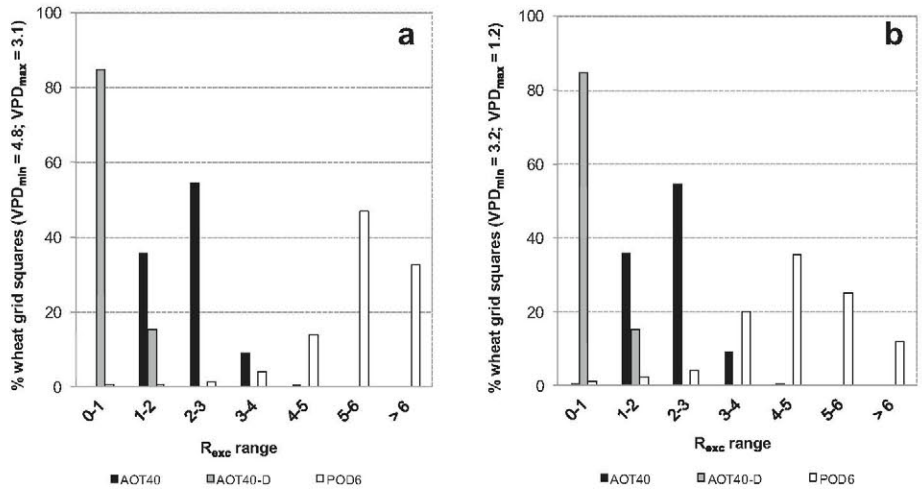

Fig. 5. Critical level exceedance for wheat. Percentage of grid squares per range of R_{exc} for wheat – VPD_{max} = 3.1 kPa and VPD_{min} = 4.8 kPa – (a) and percentage of grid squares per range of R_{exc} for wheat – VPD_{max} = 1.2 kPa and VPD_{min} = 3.2 kPa – (b).

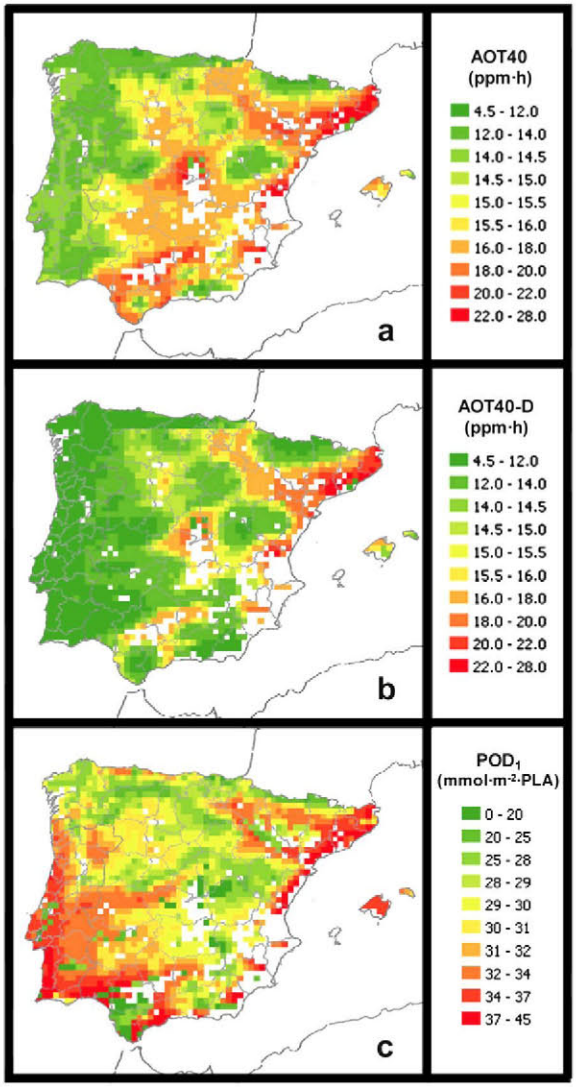

Fig. 6. Distribution of AOT40 (a), AOT40-D (b) and POD_1 (c) values during 2007 in the Iberian Peninsula for Holm oak.

press). The results obtained using the standard $VPD_{max} = 1.2$ kPa and $VPD_{min} = 3.2$ kPa values (LRTAP Convention, 2010, Table 3.10) are presented in Fig. 4f. It can be seen how the estimated POD_6 values are lower (−18% as average) than those shown in Fig. 4e, especially in the central plateaus. As shown in Fig. 5b, most of R_{exc} values range between 4 and 5 (36% of grid cells) and R_{exc} values higher than 6 are reduced to 12% of grid cells.

3.3. Holm oak

Fig. 6 shows the assessment of daylight AOT40, AOT40-D and POD_1 parameters for Holm oak. The areas that experienced the highest values of daylight AOT40 (Fig. 6a) and AOT40-D (Fig. 6b) were located in the north eastern, central and southern areas of the IP. These data are in agreement with the daylight AOT40 values reported by Sanz et al. (2000) for different areas of eastern Spain. The highest values of POD_1 (Fig. 6c) were found by the Mediterranean coast, but almost evidently around southern Portugal. The different results obtained in the centre of the IP depending on the approach followed (exposure-based or flux-based) can be explained because during summertime, when high ozone ambient concentration occur in these locations, the f_{phen} and f_{SWP} parameters reached their minimum value according to LRTAP Convention (2010) methodology and thus, the influence of these high O_3 concentrations in the POD_1 was diminished. This is in agreement with the stomatal closure performed by Holm oak during meteorological summer conditions reported by Manes et al. (2007). The three metrics consistently indicate a lower relative risk in the North western area of the IP.

Exceedances of CL were not evaluated for Holm oak. The CL defined for the classical AOT40 approach for forests may not be adequate for evergreen species under Mediterranean conditions, as suggested by Paoletti (2006). This CL was defined from more sensitive species over a time window shorter than the whole year (LRTAP Convention, 2010). According to flux-based results obtained, expose-based metrics would fail to identify high risk areas for wheat and Holm oak located in Portugal.

3.4. Effect of the Soil Moisture Content (SMC)

Fig. 7 shows the effect of SMC in the results obtained following the flux-based approach for wheat and Holm oak. Regarding wheat, differences ($SMC_{effect} > 0$) were widely found throughout the domain when SMC was taken into account (51% of grid cells). In most of these cases (86% grid cells) the differences were lower than the CL, i.e. SMC_{effect} ranged between 0 and 1. SMC_{effect} values between 1 and 2 were found in 7% of grid cells and a SMC_{effect} higher than 6 was never reached. Regarding Holm oak, differences when SMC was taken into account were only detected in 10% of grid cells where Holm oak is present. When $SMC_{effect} > 0$, differences between 10 and 40% were commonly found (47% of grid cells) and

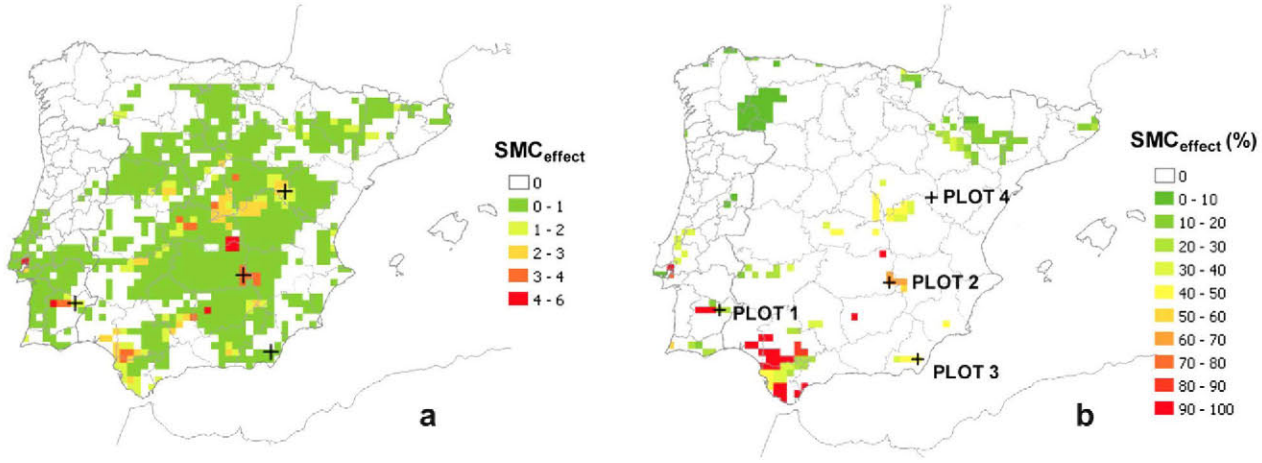

Fig. 7. Effect of soil moisture content for wheat (a) and for Holm oak (b). Locations 1, 2, 3 and 4 correspond to cells where soil moisture effect is explicitly analyzed.

Table 3
Summary of the statistical assessment of the CMAQ model performance for O_3. Values in bold corresponds to aggregated values that give an idea of average model performance better than individual values for particular locations and italics they just represent a reference standard for comparison.

INDEX[a]		AIRBASE station code												Total	Performance criteria
		PT03096	PT02020	PT02019	ES0007	ES0008	ES0009	ES0010	ES0011	ES0012	ES0013	ES0014	ES0016		
MNB (%)	$\frac{1}{N}\sum_{i=1}^{N}\left(\frac{M_i - O_i}{O_i}\right)\times 100$	2.8	5.7	4.3	12.8	0.1	0.8	1.2	7.8	2.1	7.3	0.3	8.5	**2.1**	*15*
MNE (%)	$\frac{1}{N}\sum_{i=1}^{N}\left(\frac{\lvert M_i - O_i\rvert}{O_i}\right)\times 100$	17.6	20.5	18.3	17.3	17.9	14.8	15.0	21.5	16.4	15.9	18.4	24.0	**18.2**	*35*
MFB (%)	$\frac{1}{N}\sum_{i=1}^{N}\frac{(M_i - O_i)}{(M_i + O_i)/2}$	0.2	2.5	1.9	15.4	2.4	0.9	0.5	4.2	0.0	9.5	3.4	3.6	**−0.6**	*30*
MFE (%)	$\frac{1}{N}\sum_{i=1}^{N}\frac{\lvert M_i - O_i\rvert}{(M_i + O_i)/2}$	16.6	19.2	17.5	19.5	17.8	14.6	14.7	19.6	16.4	16.8	17.7	20.9	**17.5**	*45*
IOA	$1 - \frac{\sum_{i=1}^{N}(M_i - O_i)^2}{\sum_{i=1}^{N}\lvert\lvert M_i - \overline{M}\rvert + \lvert O_i - \overline{O}\rvert\rvert^2}$	0.86	0.75	0.84	0.71	0.80	0.79	0.85	0.75	0.81	0.81	0.86	0.80	**0.81**	*0.65*
R	$\frac{\sum_{i=1}^{N}(M_i - \overline{M})\times(O_i - \overline{O})}{\left[\sqrt{\sum_{i=1}^{N}(M_i - \overline{M})^2}\right]\times\left[\sqrt{\sum_{i=1}^{N}(O_i - \overline{O})^2}\right]}$	0.74	0.57	0.72	0.60	0.67	0.65	0.76	0.57	0.65	0.71	0.76	0.66	**0.68**	*0.65*
RDE (%)	$\frac{\lvert O_{1V} - M_{1V}\rvert}{1V}\times 100$	3.6	5.1	7.1	7.0	17.0	8.8	15.5	8.5	7.7	0.9	1.4	6.9	**21.2**	*50*

[a] INDEXES: MNB — Mean Normalized Bias; MNE — Mean Normalized Error; MFB — Mean Fractional Bias; MFE — Mean Fractional Error; IOA — Index of agreement; *R* — Correlation coefficient; RDE — Relative Directive Error (Directive 2008/50/EC).

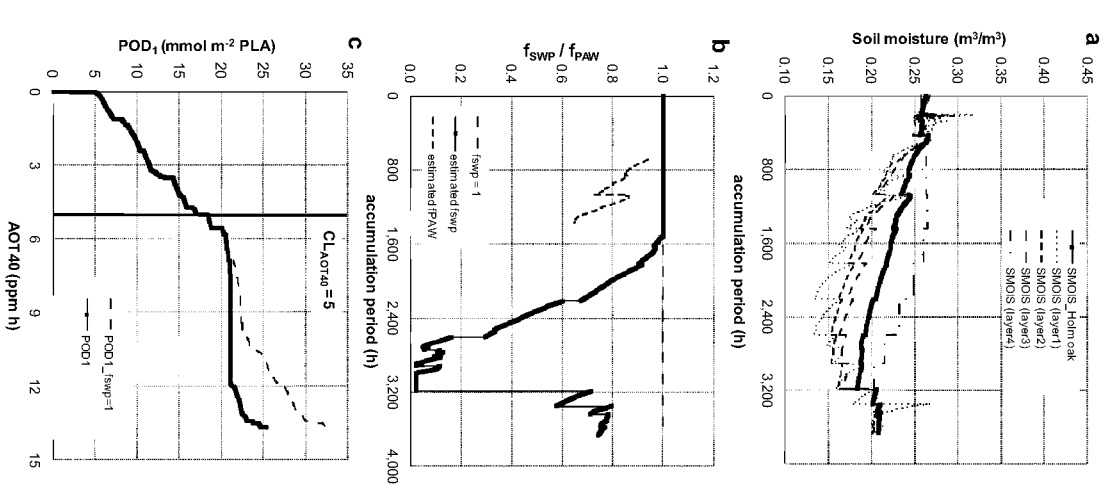

Fig. 8. Effect of soil moisture content during the accumulation period in location 1 (C13_RF21). Soil moisture in each of the four soil layers and weighted value for Holm oak (a), estimated values of f_{PAW} and f_{SWP} (b), evolution of AOT40, POD_1 and $POD1\_fswp = 1$ (POD_1 neglecting SMC) (c).

SMC_{effect} values between 90 and 100% were observed in the south of Spain (14% of grid cells). These results are closely related to the effect of drought on the stomata closure in some areas (f_{SWP} equal or close to f_{min} during most of the accumulation period which means low ozone stomatal uptake).

As for the four locations analyzed in detail, drought effect was clear in the POD_1 evolution at location 1 (Fig. 8c). During the first

part of the accumulation period, under humid conditions ($f_{SWP} = 1$, Fig. 8b), POD_1 and AOT40 evolved linearly, as previously observed by Baumgarten et al. (2009). When water shortage began, POD_1 stagnated upon stomatal closure while AOT40 kept growing. Only after post summer precipitations the SMC increased and a linear POD_1-AOT40 evolution was observed again. Even when no SMC effect was supposed (Fig. 8c, POD1_fswp = 1) there was a slow-down in the ozone uptake during summer. This can be explained by the effect of f_{phen}, f_{temp} and f_{VPD} over stomatal conductance. As Fig. 8b shows, f_{PAW} evolved under f_{SWP} during the accumulation

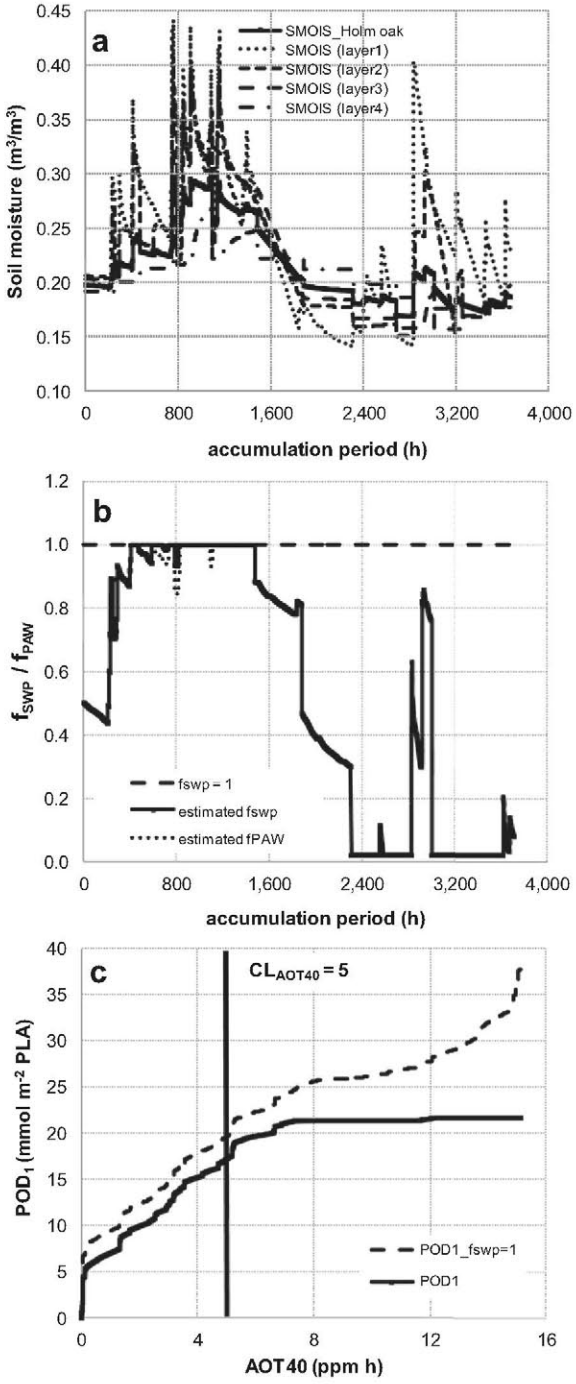

Fig. 9. Effect of soil moisture content during the accumulation period in location 3 (C41_RF14). Soil moisture in each of the four soil layers and weighted value for Holm oak (a), estimated values of f_{PAW} and f_{SWP} (b), evolution of AOT40, POD_1 and POD1_$f$swp = 1 (POD_1 neglecting SMC) (c).

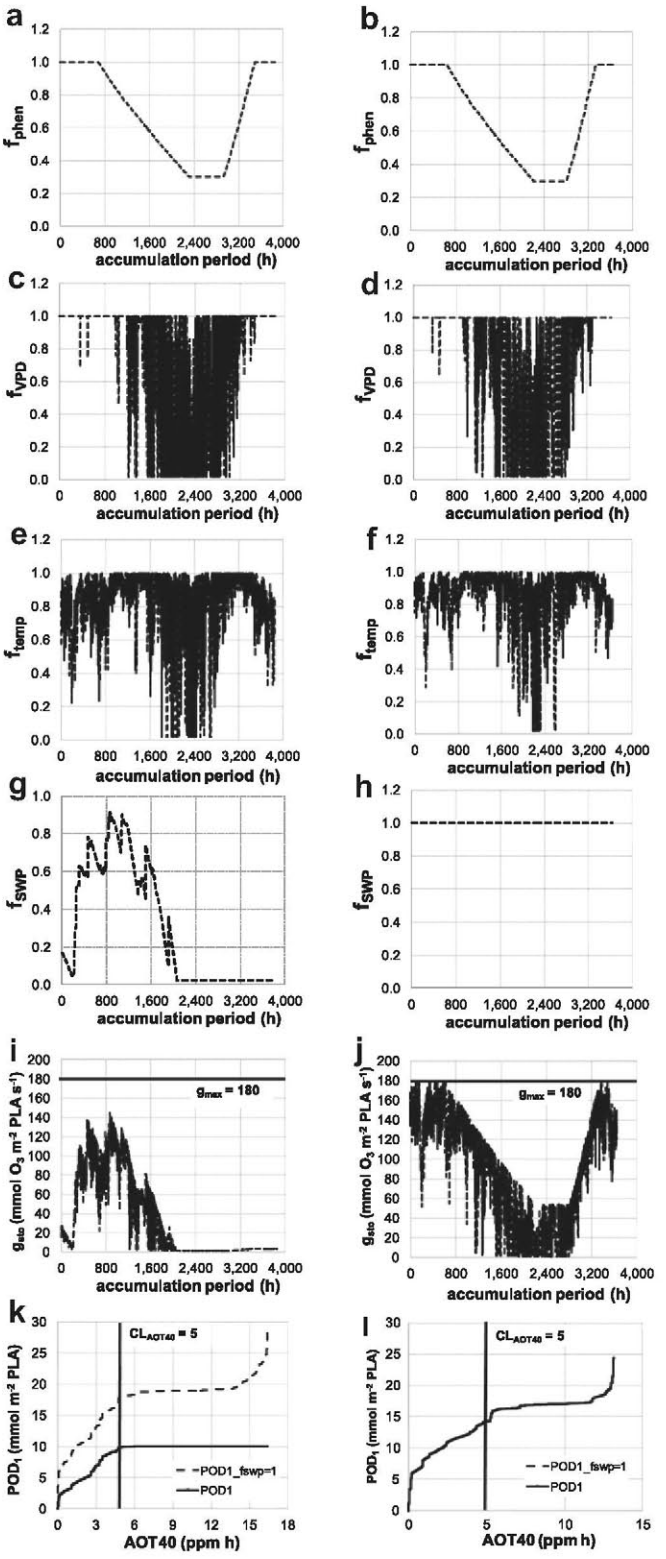

Fig. 10. Evolution during the accumulation period of most of the main parameters used in the determination of stomatal uptake. Evolution of f_{phen} (a), f_{VPD} (c), f_{temp} (e), f_{SWP} (g), g_{sto} (i) and evolution of AOT40, POD_1 and POD1_$f$swp = 1 (k) in location 2 (C37_RF25). Evolution of f_{phen} (b), f_{VPD} (d), f_{temp} (f), f_{SWP} (h), g_{sto} (j) and evolution of AOT40, POD_1 and POD1_$f$swp = 1 (l) in location 4 (C43_RF37).

period for wheat. It can be partially explained by the fact that SMC values in the tree first soil layers (used to estimate f_{PAW}) were lower than weighted SMC for Holm oak (estimated throughout all the soil profile) (Fig. 8a).

Different results were found in location 3 (Fig. 9). As it can be seen in Fig. 9b, f_{PAW} values were quite similar to those of f_{SWP} because the weighted SMC of the tree first soil layers was close to the weighted SMC for the whole soil profile. As far as comparison between POD_1 and AOT40 was concerned, two different evolutions were observed. From March to the beginning of June, the SMC was high (f_{SWP} close to 1) and a linear relationship between POD_1 and AOT40 was observed. Later, during summertime, SMC decreased and consequently only AOT40 increased. In this case, although there was an increase of f_{SWP} in September–October, the POD_1 kept almost invariant. Important differences would be found at this particular location if SMC was not taken into account (SMC_{effect} close to 42%).

Fig. 10 shows the information regarding locations 2 and 4. Throughout half of the accumulation period, meteorological and SMC conditions produced virtually nil values of g_{sto} in location 2 (Fig. 10i). As a result, POD_1 stagnated at 10 mmol m^{-2} PLA whereas AOT40 reached a value of 16.4 ppm h (Fig. 10k). Important differences (SMC_{effect} of 64%) arose when no water limitations were assumed ($POD1\_fswp = 1$, Fig. 10k).

On the other hand, water shortage was not detected in location 4 (Fig. 10h). It can be seen how POD_1 and AOT40 evolved linearly until June (Fig. 10l). During summertime (July–September) there was a slowdown in the POD_1 increase due to the phenological and environmental limitations. After September, there was a first period where the POD_1 and AOT40 increased linearly again followed by an increase of only POD_1 value at the end of the accumulation period. Obviously, POD_1 and $POD1\_fswp = 1$ are coincident in this case.

4. Conclusions

The implementation and application of a module to estimate risks of ozone damage to vegetation in the Integrated Assessment Modelling (IAM) system for the Iberian Peninsula (IP) revealed policy-relevant differences among concentration-based and flux-based assessment methods due to the particular climatic characteristics of the IP.

Exposure-based metrics (AOT40 and AOT40-D) indicated that the highest risk of ozone damage to wheat is found in the North eastern and eastern areas of the IP. Oppositely, the flux-based (POD_6) assessment revealed high ozone uptakes in the North east of the IP and in Portugal. Similar spatial distribution patterns depending on the approach followed were found to Holm oak.

In the whole IP, general exceedances of the CL were found for wheat when daylight AOT40 and POD_6 were used. On the contrary, almost no exceedances of target values (TV) were detected with AOT40-D. According to the exposure and dose response functions included in LRTAP Convention (2010), the highest values of daylight AOT40 and POD_6 in the modelling domain would imply yield losses of up to 20 and 30%, respectively.

None of the exposure-based approaches can properly reproduce high-risk areas identified by the flux-based method in Portugal. Therefore, the use of the AOT40 methods may lead to policy recommendations that may fail to protect wheat and Holm oak located in this particular area.

According to these results, the daylight AOT40 constitutes a more conservative index than the AOT40-D for wheat since R_{exc} values obtained for daylight AOT40 are generally higher. It implies than wide areas of the IP might be being under protected when the target values included in the legislation to protect the vegetation are used. AOT40 results in areas with strong water deficit (e.g. some areas in central Spain) may indicate unrealistically high ozone risks when compared with flux-based results.

Soil Moisture Content (SMC) seems to be a critical factor to be taken into account in the computation of the flux-based approach for wheat and for Holm oak in the IP. As far as wheat was concerned, SMC had a widely spread influence on the results, reaching more than 3 times the CL in some locations. Although in more restricted areas, SMC effect for Holm oak was found to be relevant, especially in the southern area of the IP.

These findings highlight the importance of flux-based approaches as a complement to the static exposure approach followed in the European legislation when evaluating potential negative impacts of tropospheric ozone on both crops and natural vegetation.

This study constitutes a step forward for the IAM activities in Spain. In the future, the system should be refined and expanded to perform assessments for a wider variety of plants (e.g. Aleppo pine, Beech) considering specific mitigation options or future-year scenarios. In addition, further analyses are needed to understand the sensitivity and uncertainties involved in the methodology presented (e.g. resolution, hypothesis and methods used for the estimation of SMC) and its implications in the decision making process needed to provide an effective protection of the vegetation in the IP.

Acknowledgements

This study is developed under research contract 026/2006/3.12.1 of the Spanish Ministry of Environment (MARM) in the framework of the National Plan of Scientific Research, Development and Technological Innovation 2004–2007. The CMAQ modelling system was made available by the US EPA and it is supported by the Community Modelling and Analysis System (CMAS) Center. The authors acknowledge the use of emission datasets and monitoring data from the Dirección General de Calidad y Evaluación Ambiental of the MARM and the Portuguese Ministry of Environment. Reviewer's thorough review and fruitful commentaries are acknowledged as well.

References

Alonso, R., Bermejo, V., García, P., González, A., Gimeno, B.S., 1999. Assessment of soil moisture as a regulator of ozone impact on wheat grown in Central Spain. In: Fuhrer, J., Achermann, B. (Eds.), Critical Levels for Ozone-Level II. Environmental Documentation No. 115. Swiss Agency for Environment, Forest and Landscape, Bern, Switzerland, pp. 243–248.

Alonso, R., Elvira, S., Sanz, M.J., Gerosa, G., Emberson, L.D., Bermejo, V., Gimeno, B.S., 2008. Sensitivity analysis of a parameterization of the stomatal component of the DO_3SE model for Quercus ilex to estimate ozone fluxes. Environmental Pollution 155, 473–480.

Appel, W., Gilliland, A., Sarwar, G., Gilliam, R.C., 2007. Evaluation of the Community multiscale air quality (CMAQ) model Version 4.5: sensitivities impacting model performance: part I – ozone. Atmospheric Environment 41, 9603–9613.

Ashmore, M.R., 2005. Assessing the future global impacts of ozone on vegetation. Plant, Cell and Environment 28, 949–964.

Atkinson, R., 2000. Atmospheric chemistry of VOCs and NOx. Atmospheric Environment 34, 2063–2101.

Baumgarten, M., Huber, C., Büker, P., Emberson, L., Dietrich, H.-P., Nunn, A.J., Heerdt, C., Beudert, B., Matyssek, R., 2009. Are Bavarian Forests (southern Germany) at risk from ground-level ozone? Assessment using exposure and flux based ozone indices. Environmental Pollution 157, 2091–2107.

Benedictow, A., Berge, H., Fagerli, H., Gauss, M., Jonson, J.E., Nyíri, A., Simpson, D., Tsyro, S., Valdebenito, A., Shamsudheen, S.V., Wind, P., Aas, W., Hjellbrekke, A.-G., Mareckova, K., Wankmüller, R., Iversen, T., Kirkevag, A., Seland, O., Haugen, J.E., Mills, G., 2010. Transboundary Acidification, Eutrophication and Ground Level Ozone in Europe in 2008. EMEP Status Report 1/2010, ISSN 1504–6192 (online). The Norwegian Meteorological Institute, Oslo, Norway.

Bey, I., Jacob, D.J., Yantosca, R.M., Logan, J.A., Field, B.D., Fiore, A.M., Li, Q., Liu, H.Y., Mickley, L.J., Schultz, G., 2001. Global modeling of tropospheric chemistry with assimilated meteorology: model description and evaluation. Journal of Geophysical Research 106 (D19), 23073–23096.

Boldo, E., Linares, C., Lumbreras, J., Borge, R., Narros, A., García-Pérez, J., Fernández-Navarro, P., Pérez-Gómez, B., Aragonés, N., Ramis, R., Pollán, M., Moreno, T.,

Karanasiou, A., López-Abente, G., 2011. Health impact assessment of a reduction in ambient PM2.5 levels in Spain. Environment International 37, 342–348.
Borge, R., Lumbreras, J., Rodríguez, M.E., 2008a. Development of a high-resolution emission inventory for Spain using the SMOKE modelling system: a case study for the years 2000 and 2010. Environmental Modelling and Software 23, 1026–1044.
Borge, R., Alexandrov, V., del Vas, J.J., Lumbreras, J., Rodríguez, M.E., 2008b. A comprehensive sensitivity analysis of the WRF model for air quality applications over the Iberian Peninsula. Atmospheric Environment 42, 8560–8574.
Borge, R., Lumbreras, J., De La Paz, D., Rodríguez, M.E., 2009. Air quality modelling: bridging national and continental scales. In: The 18th World IMACS/MODSIM Congress, Cairns, Australia 13–17 July 2009. Available online at: http://www.mssanz.org.au/modsim09/F10/borge.pdf.
Borge, R., López, J., Lumbreras, J., Narros, A., Rodríguez, M.E., 2010. Influence of boundary conditions on CMAQ simulations over the Iberian Peninsula. Atmospheric Environment 44, 2681–2695.
Brankov, E., Henry, R.F., Civerolo, K.L., Hao, W., Rao, S.T., Misra, P.K., Bloxam, R., Reid, N., 2003. Assessing the effects of transboundary ozone pollution between Ontario, Canada and New York, USA. Environmental Pollution 123, 403–411.
Byun, D.W., Ching, J.K.S., 1999. Science Algorithms of the EPA Models-3 Community Multi-scale Air Quality (CMAQ) Modeling System. EPA/600/R-99/030, US EPA National Exposure Research Laboratory, Research Triangle Park, NC.
Byun, D.W., Schere, K.L., 2006. Review of the governing equations, computational algorithms, and other components of the Models-3 community Multiscale Air Quality (CMAQ) modeling system. Applied Mechanics Reviews 59, 51–77.
Chen, F., Dudhia, J., 2001a. Coupling and advanced land surface-hydrology model with the Penn State-NCAR MM5 modeling system. Part I. Model implementation and sensitivity. Monthly Weather Review 129, 569–585.
Chen, F., Dudhia, J., 2001b. Coupling an advanced land surface-hydrology model with the Penn-State-NCAR MM5 modeling system. Part II. Preliminary model validation. Monthly Weather Review 129, 587–604.
Chen, X., Hu, Q., 2004. Groundwater influences on soil moisture and surface evaporation. Journal of Hydrology 297, 285–300.
Delgado-Saborit, J.M., Esteve-Cano, V.J., 2008. Assessment of tropospheric ozone effects on citrus crops using passive samplers in a western Mediterranean area. Agriculture, Ecosystems & Environment 124, 147–153.
Denby, B., Sundvor, I., Cassiani, M., de Smet, P., de Leeuw, F., Horálek, J., 2010. Spatial mapping of ozone and SO_2 trends in Europe. Science of the Total Environment 408, 4795–4806.
Dueñas, C., Fernández, M.C., Cañete, S., Carretero, J., Liger, E., 2002. Assessment of ozone variations and meteorological effects in an urban area in the Mediterranean Coast. Science of the Total Environment 299, 97–113.
Elvira, S., Bermejo, V., Manrique, E., Gimeno, B.S., 2004. On the response of two populations of Quercus coccifera to ozone and its relationship with ozone uptake. Atmospheric Environment 38, 2305–2311.
Emberson, L.D., Ashmore, M.R., Cambridge, H.M., Simpson, D., Tuovinen, J.-P., 2000. Modelling stomatal ozone flux across Europe. Environmental Pollution 109, 403–413.
EEA, 2010. Air Pollution by Ozone Across Europe During Summer 2009 (EEA Technical Report No. 2/2010). European Environment Agency. ISSN 1725-2237. Available online at: http://www.eea.europa.eu/publications/air-pollution-by-ozone-across-europe-during-summer-2009.
Fuhrer, J., Skärby, L., Ashmore, M.R., 1997. Critical levels for ozone effects on vegetation in Europe. Environmental Pollution 97, 91–106.
Fuhrer, J., Booker, F., 2003. Ecological issues related to ozone: agricultural issues. Environment International 29, 141–154.
Fumagalli, B., Ambrogi, R., Mignanego, L., 1999. Ozone in southern Europe: UN/ECE experiments in Italy suggest a new approach to critical levels. In: Fuhrer, J., Achermann, B. (Eds.), Critical Levels for Ozone-Level II. Environmental Documentation No. 115. Swiss Agency for Environment. Forest and Landscape, Bern, Switzerland, pp. 239–242.
Fumagalli, I., Gimeno, B.S., Velissariou, D., De Temmerman, L., Mills, G., 2001. Evidence of ozone-induced adverse effects on crops in the Mediterranean region. Atmospheric Environment 35, 2583–2587.
García, M.A., Sánchez, M.L., Pérez, I.A., de Torre, B., 2005. Ground level ozone concentrations at a rural location in northern Spain. Science of the Total Environment 348, 135–150.
Grell, G.A., Dudhia, J., Stauffer, D.R., 1994. A Description of the Fifth-Generation Penn State/NCAR Mesoscale Model, NCAR Technical Note NCAR/TN-398+STR, 122 pp.
ICP Vegetation, 2009. Flux-based Assessment of Ozone Effects for Air Pollution Policy. In: ICP Vegetation Expert Panel Meeting, 9–12 November 2009. JRC-ISPRA, Italy.
ICP Vegetation 2007. Hayes, F., Mills, G., Harmens, H., Norris, D., 2007. Evidence of Widespread Ozone Damage to Vegetation in Europe (1990–2006). The ICP Vegetation reports to the Working Group on Effects of the Convention on Long-range Transboundary Air Pollution.
Karlsson, P.E., Uddling, J., Braun, S., Broadmeadow, M., Elvira, S., Gimeno, B.S., Le Thiec, D., Oksanen, E., Vandermeiren, K., Wilkinson, M., Emberson, L., 2004. New critical levels for ozone effects on young trees based on AOT40 and simulated cumulative leaf uptake of ozone. Atmospheric Environment 38, 2283–2294.
Li, Q., Dong, B., Qiao, Y., Liu, M., Zhang, J., 2010. Root growth, available soil water, and water-use efficiency of winter wheat under different irrigation regimes applied at different growth stages in North China. Agricultural Water Management 97, 1676–1682.
Lilley, J.M., Kirkegaard, J.A., 2011. Benefits of increased soil exploration by wheat roots. Field Crops Research 122, 118–130.
LRTAP Convention, 2010. Manual on Methodologies and Criteria for Modelling and Mapping Critical Loads and Levels and Air Pollution Effects, Risks and Trends. In: Chapter 3, Mapping Critical Levels for Vegetation (2010 Revision). Convention on Long-range Transboundary Air Pollution. Available online at: http://icpvegetation.ceh.ac.uk/manuals/documents/Ch3revisedsummer2010final_221010_.pdf.
Lumbreras, J., Borge, R., de Andrés, J.M., Rodríguez, M.E., 2008. A model to calculate consistent atmospheric emission projections and its application to Spain. Atmospheric Environment 42, 5251–5266.
Manes, F., Vitale, M., Fabi, A.M., De Santis, F., Zona, D., 2007. Estimates of potential ozone stomatal uptake in mature trees of *Quercus ilex* in a Mediterranean climate. Environmental and Experimental Botany 59, 235–241.
Mediavilla, S., Escudero, A., 2004. Stomatal responses to drought of mature trees and seedlings of two co-occurring Mediterranean oaks. Forest Ecology and Management 187, 281–294.
Millán, M.M., Mantilla, E., Salvador, R., Carratalá, A., Sanz, M.J., 2000. Ozone cycles in the Western Mediterranean basin: interpretation of monitoring data in complex coastal terrain. Journal of Applied Meteorology 39, 487–508.
Mills, G., Buse, A., Gimeno, B., Bermejo, V., Holland, M., Emberson, L., Pleijel, H., 2007a. A synthesis of AOT40-based response functions and critical levels of ozone for agricultural and horticultural crops. Atmospheric Environment 41, 2630–2643.
Mills, G., Hayes, F., Jones, M.L.M., Cinderby, S., 2007b. Identifying ozone-sensitive communities of (semi-)natural vegetation suitable for mapping exceedance of critical levels. Environmental Pollution 146, 736–743.
Mills, G., Pleijel, H., Braun, S., Büker, P., Bermejo, V., Calvo, E., Danielsson, H., Emberson, L., González Fernández, I., Grünhage, L., Harmens, H., Hayes, F., Karlsson, P.-E., Simpson, D., 2011a. New stomatal flux-based critical levels for ozone effects on vegetation. Atmospheric Environment 45, 5064–5068.
Mills, G., Hayes, F., Simpson, D., Emberson, L., Norris, D., Harmens, H., Büker, P., 2011b. Evidence of widespread effects of ozone on crops and (semi-)natural vegetation in Europe (1990–2006) in relation to AOT40- and flux-based risk maps. Global Change Biology 17, 592–613.
Moreno, G., Obrador, J.J., Cubera, E., Dupraz, C., 2005. Fine root distribution in Dehesas of Central-Western Spain. Plant and Soil 277, 153–162.
Nussbaum, S., Remund, J., Rihm, B., Mieglitz, K., Gurtz, J., Fuhrer, J., 2003. High-resolution spatial analysis of stomatal ozone uptake in arable crops and pastures. Environment International 29, 385–392.
Paoletti, E., 2006. Impact of ozone on Mediterranean forests: a review. Environmental Pollution 144, 463–474.
Pederzoli, A., Thunis, P., Georgieva, E., Borge, R., Carruthers, D., 2011. Performance Criteria for the Benchmarking of Air Quality Model Regulatory Applications: The "Target" Approach. In: 14th International Conference on Harmonization within Atmospheric Dispersion Modelling for Regulatory Purposes. Kos (Greece), ISBN 978-960-89650-6-5.
Pleijel, H., Danielsson, H., Ojanperä, K., De Temmerman, L., Högy, P., Badiani, M., Karlsson, P.E., 2004. Relationships between ozone exposure and yield loss in European wheat and potato-a comparison of concentration- and flux-based exposure indices. Atmospheric Environment 38, 2259–2269.
Pleijel, H., Danielsson, H., Emberson, L., Ashmore, M.R., Mills, G., 2007. Ozone risk assessment for agricultural crops in Europe: further development of stomatal flux and flux–response relationships for European wheat and potato. Atmospheric Environment 41, 3022–3040.
Richards, L.A., 1931. Capillary conduction of liquids through porous mediums. Physics 1, 318–333. doi:10.1063/1.1745010.
Russell, A., Dennis, R., 2000. NARSTO critical review of photochemical models and modelling. Atmospheric Environment 34, 2261–2282.
Sanz, M.J., Carratalá, A., Mantilla, E., Diéguez, J.J., Millán, M., 1999. Daily ozone patterns and AOT40 index on the East Coast of the Iberian Peninsula. Physics and Chemistry of the Earth, Part C: Solar, Terrestrial & Planetary Science 24, 491–494.
Sanz, M.J., Calatayud, V., Sánchez-Peña, G., 2007. Measures of ozone concentrations using passive sampling in forests of South Western Europe. Environmental Pollution 145, 620–628.
Sanz, M.J., Calatayud, V., Calvo, E., 2000. Spatial pattern of ozone injury in Aleppo pine related to air pollution dynamics in a coastal-mountain region of eastern Spain. Environmental Pollution 108, 239–247.
Simpson, D., Ashmore, M.R., Emberson, L., Tuovinen, J.-P., 2007. A comparison of two different approaches for mapping potential ozone damage to vegetation. A model study. Environmental Pollution 146, 715–725.
Simpson, D., Fagerli, H., Jonson, J., Tsyro, S., Wind, P., Tuovinen, J.-P., 2003. The EMEP Unified Eulerian Model. In: Model Description, EMEP MSC-W Report 1/2003. The Norwegian Meteorological Institute, Oslo, Norway.
Shi, C., Fernando, H.J.S., Yang, J., 2009. Contributors to ozone episodes in three U.S./Mexico border twin-cities. Science of the Total Environment 407, 5128–5138.
Skamarock, W.C., Klemp, J.B., 2008. A time-split nonhydrostatic atmospheric model. Journal of Computational Physics 227, 3465–3485.
Thunis, P., Georgieva, E., Pederzoli, A., 2011. The DELTA Tool and Benchmarking Report Template. In: Concepts and User's Guide, Version 2. Available at: http://aqm.jrc.it/DELTA/data/DELTA_SG4_V2.pdf.
Tuovinen, J.-P., Ashmore, M.R., Emberson, L.D., Simpson, D., 2004. Testing and improving the EMEP ozone deposition module. Atmospheric Environment 38, 2373–2385.
UNC Carolina Environmental Program, 2005. Sparse Matrix Operator Kernel Emissions (SMOKE) Modeling System.

Xu, J., Zhang, Y., Fu, J.S., Zheng, S., Wang, W., 2008. Process analysis of typical summertime ozone episodes over the Beijing area. Science of the Total Environment 399, 147–157.

Yarwood, G., Rao, S., Yocke, M., Whitten, G., 2005. Updates to the Carbon Bond Chemical Mechanism: CB05. In: Final Report to the US EPA, RT-0400675. Available online at: http://www.camx.com/publ/pdfs/CB05_Final_Report_120805.pdf.

Zhang, L., Vet, R., Brook, J.R., Legge, A.H., 2006. Factors affecting stomatal uptake of ozone by different canopies and a comparison between dose and exposure. Science of the Total Environment 370, 117–132.